Novel water-based nanolubricant with superior tribological performance in hot steel rolling

OPEN ACCESS
IOP Publishing | IMMT
International Journal of Extreme Manufacturing
Int. J. Extrem. Manuf. **2** (2020) 025002 (11pp)
https://doi.org/10.1088/2631-7990/ab82fe

Novel water-based nanolubricant with superior tribological performance in hot steel rolling

Hui Wu[1], Fanghui Jia[1], Zhou Li[1], Fei Lin[1], Mingshuai Huo[1], Shuiquan Huang[2], Sepidar Sayyar[3,4], Sihai Jiao[5], Han Huang[2] and Zhengyi Jiang[1]

[1] School of Mechanical, Materials, Mechatronic and Biomedical Engineering, University of Wollongong, Wollongong NSW 2522, Australia
[2] School of Mechanical and Mining Engineering, The University of Queensland, Brisbane QLD 4072, Australia
[3] ARC Centre of Excellence for Electromaterials Science (ACES), Intelligent Polymer Research Institute, AIIM Facility, Innovation Campus, University of Wollongong, Wollongong, NSW 2500, Australia
[4] Australian National Fabrication Facility—Materials Node, Innovation Campus, University of Wollongong, Wollongong NSW 2500, Australia
[5] Baosteel Research Institute (R&D Centre), Baoshan Iron & Steel Co., Ltd., Shanghai 200431, People's Republic of China

E-mail: hwu@uow.edu.au, han.huang@uq.edu.au and jiang@uow.edu.au

Received 12 February 2020, revised 11 March 2020
Accepted for publication 24 March 2020
Published 27 April 2020

Abstract

Novel water-based nanolubricants using TiO_2 nanoparticles (NPs) were synthesised by adding sodium dodecyl benzene sulfonate (SDBS) and glycerol, which exhibited excellent dispersion stability and wettability. The tribological performance of the synthesised nanolubricants was investigated using an Rtec ball-on-disk tribometer, and their application in hot steel rolling was evaluated on a 2-high Hille 100 experimental rolling mill, in comparison to those without SDBS. The water-based nanolubricant containing 4 wt% TiO_2 and 0.4 wt% SDBS demonstrated superior tribological performance by decreasing coefficient of friction and ball wear up to 70.5% and 84.3%, respectively, compared to those of pure water. In addition to the lubrication effect, the suspensions also had significant effect on polishing of the work roll surface. The resultant surface improvement thus enabled the decrease in rolling force up to 8.3% under a workpiece reduction of 30% at a rolling temperature of 850 °C. The lubrication mechanisms were primarily ascribed to the formation of lubricating film and ball-bearing effect of the TiO_2 NPs.

Keywords: water-based nanolubricant, TiO_2 nanoparticle, tribological performance, hot steel rolling

(Some figures may appear in colour only in the online journal)

1. Introduction

The green manufacturing and its sustainable development are becoming increasingly important in the field of manufacturing engineering, such as rolling of steels [1]. Friction and wear inevitably occur during rolling process, which leads to loss of energy and wear of work rolls [2–4]. Lubricants, including traditional neat oils [5–7] and oil-in-water emulsions [8, 9],

have thus been applied to solve these issues due to their excellent lubricating properties. The use of oil-containing lubricants, however, unavoidably generates contamination to the environment, especially when burnt and discharged [6]. Therefore, it is desirable to develop high-performance green lubricants to substitute the traditional ones. In this regard, application of nanotechnology provides an orientation to develop candidate lubricants. Among all the options, one practical way is to reduce the oil percentage in the oil-based lubricants by adding nanoparticles (NPs) as compensation [10–12]. Although the coefficient of friction (COF) and wear of tools can be decreased significantly because of the contribution of the NPs, the presence of oil still poses environmental hazards and recycling issues. In view of these disadvantages, water-based lubricants are expected to serve as potential alternatives, and they behave not only as lubricants but also as coolants for tools.

It is acknowledged that water has poor lubricity due to its insufficient film thickness. Adding nanomaterials into water has become a promising approach to enhance the lubricity of water. The cooling ability of water can also be improved by this way [13]. These nanomaterials include metals [14, 15], metallic oxides [16–18], nonmetallic oxides [19, 20], metal sulphides [21, 22], ceramics [23–25], composites [26–30] and carbon materials [31–34]. Specifically, it has been reported that metal oxides account for the largest proportion at 26% in the statistics of NPs served as lubricant additives [35]. Of all these nanoadditives, nano-TiO_2, as one of the best candidate nanomaterials, has drawn significant attention, owing to its low cost, nontoxicity, superior dispersion stability in base lubricant, excellent lubrication performance, and practical potential in the engineering applications [36]. However, the tribological performance and load-carrying capacity of current water-based TiO_2 nanolubricant need to be further improved, especially when used in steel rolling under heavy loads.

In our previous studies, the tribological behaviour of water-based nanolubricants containing TiO_2 NPs on smooth, rough and oxidised steel surfaces have been investigated under different testing conditions [36–38]. In order to further enhance their comprehensive lubricating properties and performance, water-based nanolubricants with innovatively optimised formula were proposed in present study. Their application in hot steel rolling was then examined, and corresponding lubrication mechanisms were discussed.

2. Experimental details

2.1. Materials

A ball made of E52100 chrome steel and a low-alloy steel disk (namely Q345 with yield stress of 345 MPa) were used as a friction pair in a ball-on-disk tribometer. The ball represented the roll material, while the disk represented the strip steel. The chemical compositions of these two materials are listed in table 1. The balls being used had a diameter of 9.5 mm and a surface roughness of 0.02 μm in R_a. The disks were machined to a dimension of Φ40 mm $\times$ 8 mm with a surface roughness of 0.14 μm in R_a. The Vickers hardness values of the ball and disk are around 780 and 160 HV, respectively. Surface morphologies and 3D profiles of the friction pair are displayed in figure 1. It can be seen that the ball surface is relatively smooth, while the disk surface possesses apparent scratches. The rough surfaces were obtained to represent the actual surface conditions of steels [39].

Table 1. Chemical compositions of the ball and disk materials (wt%).

Materials	C	Si	Mn	Cr	Cu	Ni	Mo	Nb + V + Ti
Ball-E52100	1.0	0.25	0.35	1.5	0.3	0.2	0.1	—
Disk-Q345	0.16	0.25	1.5	0.02	0.01	0.006	0.007	< 0.02

The steel Q345 was also used as workpiece in hot rolling test. Before each test, the workpiece was machined to dimensions of 300 (length) $\times$ 91 (width) $\times$ 8.5 (thickness) mm^3 with a tapered edge for an easy roll bite. Both sides of the workpiece were then ground and polished to generate identical surfaces with a roughness of 0.5 μm in R_a. Later on, the workpiece was cleaned with acetone to remove any residuals retained from machining.

The novel water-based nanolubricants being used in this study are composed of TiO_2 NPs (type P25), SDBS, glycerol and distilled water. P25 is a mixture that contains 75% of anatase and 25% of rutile with approximately 20 nm in diameter [38]. SDBS is an organic dispersant with hydrophilic group to improve the dispersion stability, wettability and viscosity of the nanolubricants [40–42]. Glycerol is a colorless, odorless and viscous liquid that facilitates the enhancement of suspension viscosity [43]. The synthesis procedure of the water-based nanolubricants can be found elsewhere, showing excellent dispersion stability [44]. The chemical compositions of the applied nanolubricants are shown in table 2. For comparison purpose, distilled water and the nanolubricants without SDBS were also used.

2.2. Tribological and rolling tests

An Rtec MFT-5000 Multi-functional Tribometer was used to evaluate the tribological performance of applied lubricants under the ball-on-disk tribo-testing configuration (see figure 2). The COF and the wear of ball were thus obtained after each test. This configuration was consistent to that reported in our previous study [36] where the disk surface was covered by a layer of lubricant with a fixed volume of 2 ml prior to each tribological test. By doing this, the initial conditions of the tribological tests can be well controlled. Both the ball and disk were cleaned in an ultrasonic ethanol bath for 2 min before and after each test. The tribo-testing conditions employed are listed in table 3. Varying loads of 20, 30, 50 and 80 N were applied on the ball to slide against the rotating disk for a period of 10 min. The linear speed and radius of the wear track were 50 mm s^{-1} and 14 mm, respectively. It is worth noticing that a relatively low sliding speed hereby was adopted to minimise the hydrodynamic effect on the testing results [37]. The time histories of COF were recorded during testing, and the wear of ball was then evaluated after the test. For each

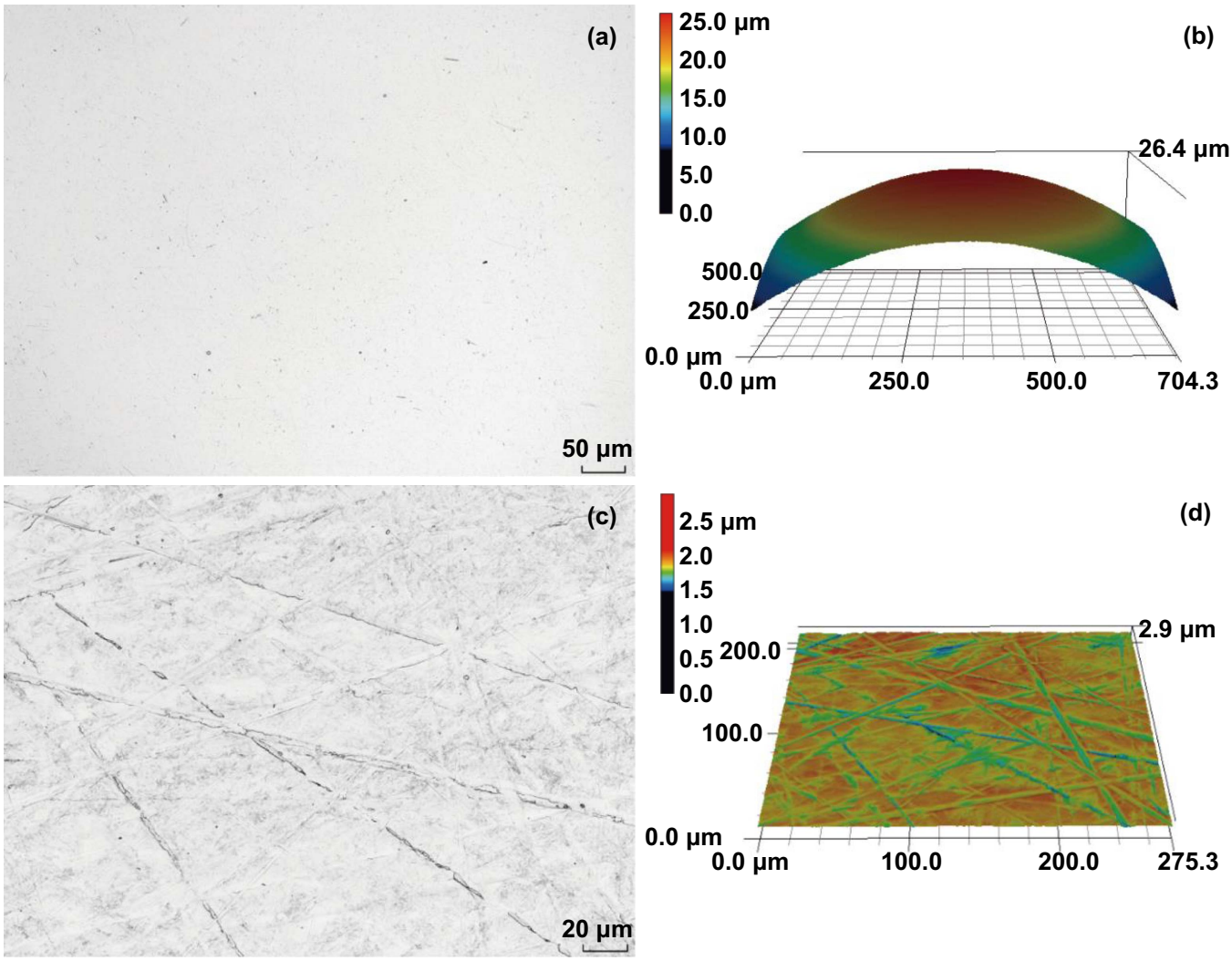

Figure 1. Surface morphologies and 3D profiles of (a), (b) E52100 Cr steel ball, and (c), (d) Q345 disk.

Table 2. Chemical compositions of applied lubricants.

Lubrication type	Description
W	Distilled water
A	2.0 wt% TiO_2 + 10 wt% glycerol + balance water
B	4.0 wt% TiO_2 + 10 wt% glycerol + balance water
C	2.0 wt% TiO_2 + 10 wt% glycerol + 0.2 wt% SDBS + balance water
D	4.0 wt% TiO_2 + 10 wt% glycerol + 0.4 wt% SDBS + balance water

condition, the same test was conducted three times to ensure repeatability.

Beside the tribological tests, the effectiveness of all the lubricants was assessed during hot steel rolling on a 2-high Hille 100 experimental rolling mill. The work roll has a dimension of Φ225 mm × 254 mm and a surface roughness of 2.88 μm in R_a. The Q345 workpieces were heated in a high-temperature electric resistance furnace at 900 °C for a soaking period of 30 min inside an atmosphere of nitrogen. The hot workpieces were then rolled at an estimated temperature of 850 °C with a reduction of 30% and a rolling speed of 0.35 m s^{-1} under different lubrication conditions as mentioned in table 2. After rolling, the steel strips were cooled down in air. As described in the previous studies [43–45], the distilled water and water-based nanolubricants were sprayed onto the pre-cleaned work roll surfaces prior to each rolling test until a uniform and saturated layer of liquid film was formed. Each hot rolling test was performed three times to minimise data scattering of rolling force, and average values were thus obtained.

2.3. Analytical techniques

The dispersion stability of as-synthesised water-based nanolubricants was evaluated using a UV-1800 ultraviolet visible (UV–vis) spectrophotometer. The UV intensities of the nanolubricants were measured in terms of the NP sedimentation rate. The relative concentration was calculated by the ratio between the initial intensity of NP concentration and the following intensity on different days.

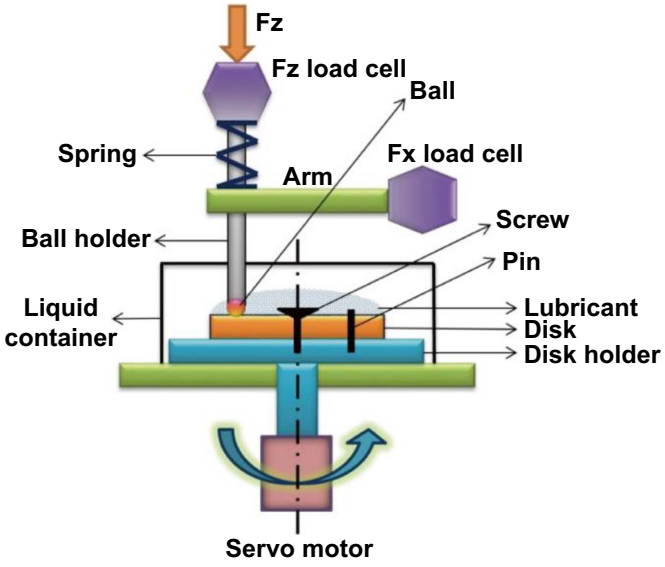

Figure 2. Schematic diagram of the ball-on-disk configuration used for tribological test.

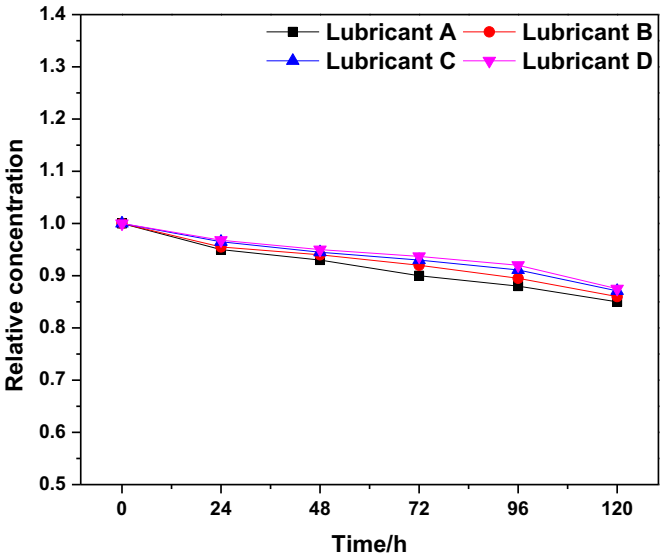

Figure 3. Dispersion stability of various water-based nanolubricants evaluated by using UV–vis spectrophotometer within 5 d.

Table 3. Tribo-testing conditions at room temperature.

Load	Linear speed	Radius of wear track	Duration
20, 30, 50 and 80 N	50 mm s^{-1}	14 mm	10 min

The dynamic viscosity of as-synthesised water-based nanolubricants was measured at room temperature using a rheometer (AR-G2 TA Instrument) with a stainless steel cone-plate which had a geometry of 40 mm in diameter. The shear rate used for viscosity measurement was 0.1 to 1000 s^{-1}. Each measurement was conducted at least three times to ensure repeatability.

Wear scars of the balls generated after the tribological tests were observed under a KEYENCE VK-X100 K 3D Laser Scanning Microscope. The wear of ball was evaluated by the calculation of wear scar areas. Wear tracks of the disks were observed using a JSM-7001 F Scanning Electron Microscope (SEM) equipped with an energy dispersive spectrometer (EDS) to investigate the lubrication mechanisms.

The rolling force data was recorded during hot rolling using two individual load cells assembled at the drive and operation sides on the rolling mill. The data acquisition was completed via MATLAB xPC technology (2009).

The wettability of the lubricants was characterised by the measurement of contact angles using a Rame-hart 290 Goniometer. The lubricant microdroplets that spread on the surface of roll material (high speed steel, abbreviated as HSS) were observed with an amplified profile projection, followed by an angulation in the affiliated software.

3. Results

3.1. Dispersion stability

Figure 3 shows the dispersion stability of the synthesised water-based nanolubricants in a period of 5 d. It is noted that the relative concentration at 1.0 indicates perfect stability of the nanolubricants without particle sedimentation. For lubricant A, the relative absorption drops continuously until it reaches around 85% on the fifth day. In contrast, the relative absorption in lubricant B declines a bit more slowly than that of lubricant A, suggesting better stability. With the addition of SDBS into lubricants A and B, by comparison, lubricants C and D exhibit higher relative adsorption on each day, and the final value is over 87% after standing for 5 d. It is also evidently shown that the dispersion stability of lubricant D is superior to that of lubricant C. These results reveal that all the as-synthesised water-based nanolubricants demonstrate excellent dispersion stability within 120 h, and the stabilisation of the nanolubricants with SDBS can be greatly improved.

3.2. Coefficient of friction

Figure 4(a) shows the COF curves over sliding time under different lubrication conditions. It can be seen that the use of distilled water enables a COF curve with significant fluctuation throughout the entire sliding process, and the COF curve begins to maintain at a stable level after a running-in period of 300 s. In contrast, the COF curve generated using lubricant A exhibits a lower level with much smaller fluctuation than those of water, and it continues to decline with lubricant B being used. Meanwhile, the running-in period is shortened from 300 to 150 s. The COF level can be further lowered down significantly under lubricants C and D, demonstrating minor fluctuations after a running period of 50 s. The variations of averaged COF values from the stable stages of the COF curves are shown in figure 4(b). It is found that water presents the highest COF value of 0.356, which can be reduced continuously by using lubricants A and B. The use of lubricants C and D, by contrast, can further reduce the COF to an even larger extent, suggesting super-low COF values at around 0.1. It is worth noting that lubricant D appears to trigger a slightly lower COF

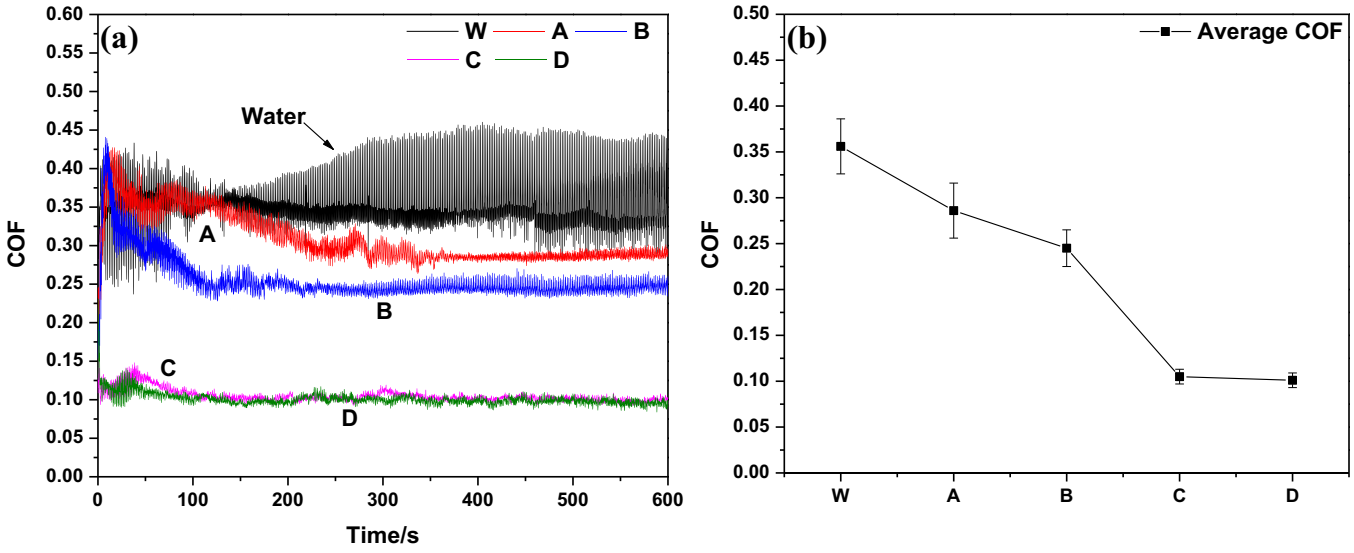

Figure 4. (a) COF curves over sliding time, and (b) averaged COF values obtained from the stable stages of sliding against Q345 disk under different lubrication conditions (30 N, 50 mm s^{-1}, 10 min).

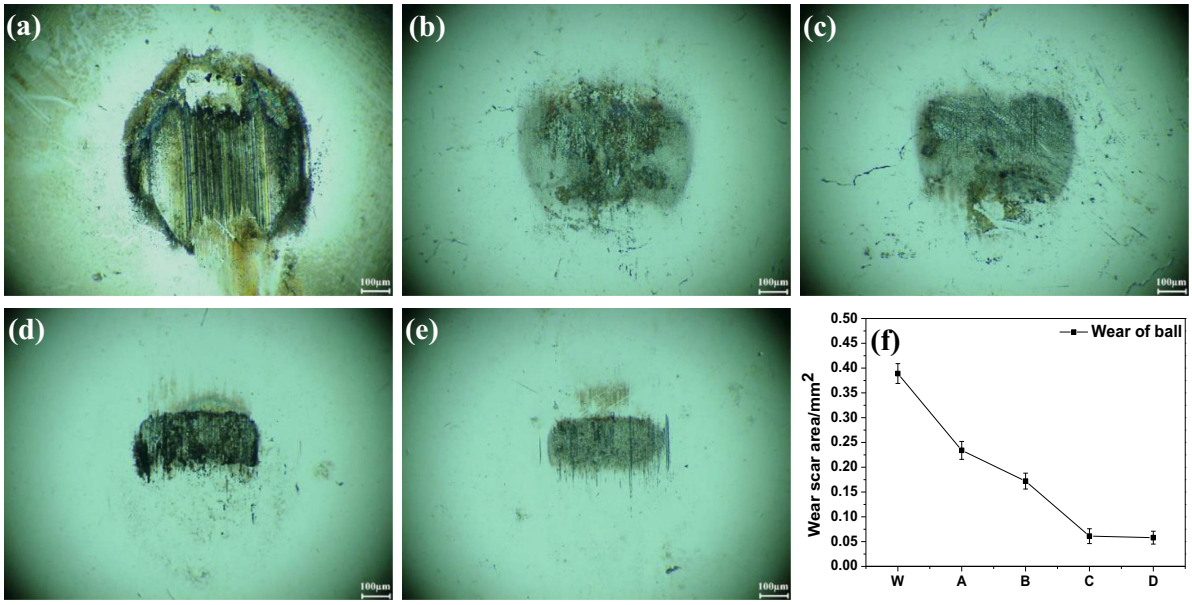

Figure 5. Surface morphologies of the worn balls obtained under (a) water, (b) lubricant A, (c) lubricant B, (d) lubricant C, (e) lubricant D, and (f) comparison of averaged wear scar areas (30 N, 50 mm s^{-1}, 10 min).

than that of lubricant C, which therefore maximally reduces the COF of water by 70.5%.

3.3. Wear of ball

Figures 5(a)–(e) show the surface morphologies of the worn balls obtained under different lubrication conditions. It can be observed that all the wear scars are elliptical, and they have continually decreasing scratches with the water-based nanolubricants being used. The corresponding wear scar areas (WSA) of the balls are averaged and shown in figure 5(f). It is evident that the variation trend of WSA is consistent with that of COF (see figure 4(b)), indicating that the ball wear caused by water can be reduced up to 84.3%. From figures 4(b) and 5(f), it can also be found that lubricant B outperforms lubricant A in terms of tribological performance. Additionally, lubricants C and D with SDBS are superior to lubricants A and B without SDBS according to decreased COF and ball wear.

3.4. Load-carrying capacity

In consideration of exceptional tribological performance of lubricant D, it is of great significance to investigate its load-carrying capacity under increasing normal loads. It can be seen in figure 6(a) that all the COF curves coincide perfectly with each other under varying loads from 20 to 80 N throughout the whole sliding process. The averaged COF values remain

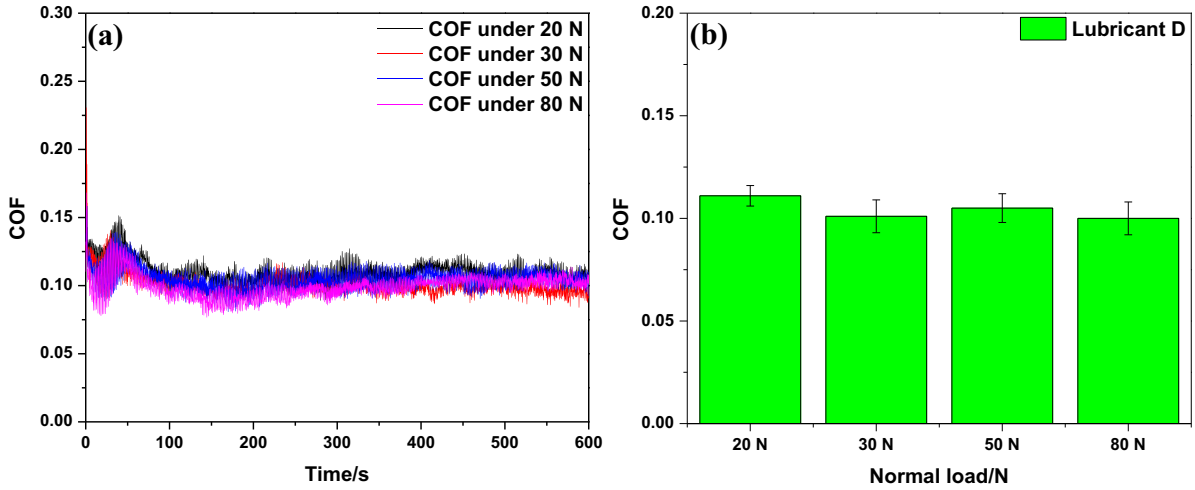

Figure 6. (a) COF curves over sliding time, and (b) averaged COF values obtained from the stable stages of sliding against Q345 disk under different loads (50 mm s^{-1}, 10 min).

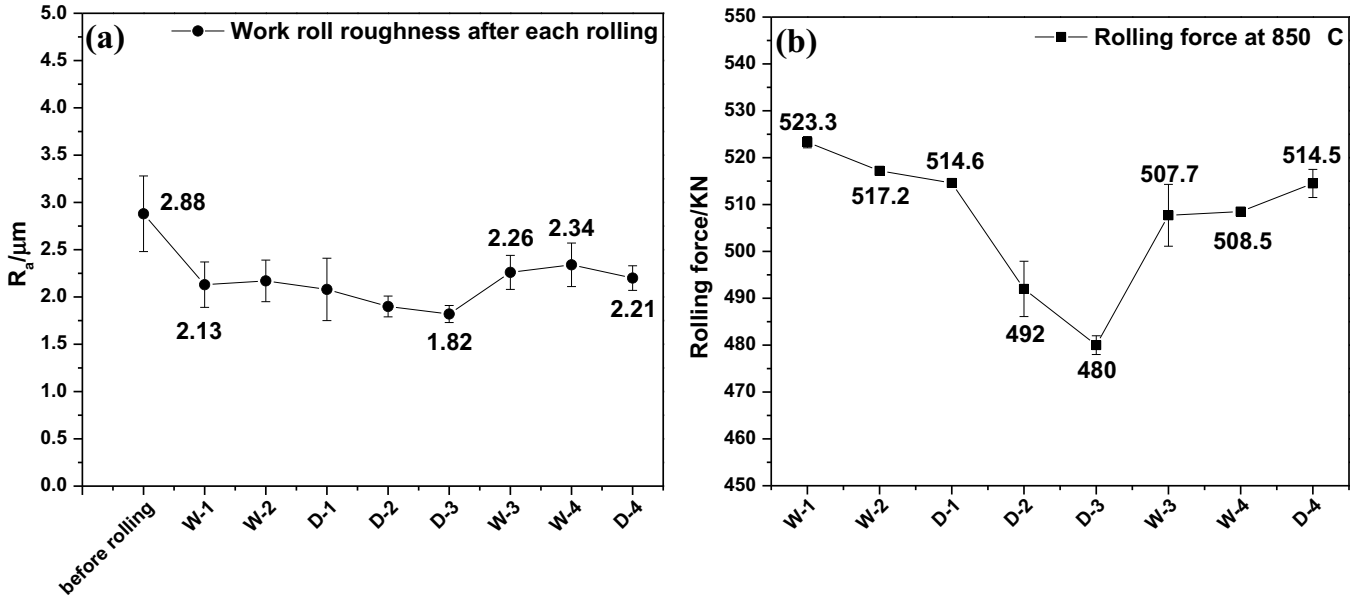

Figure 7. Variations of (a) work roll roughness and (b) corresponding rolling force under water and lubricant D at 850 °C.

almost constant at approximately 0.1 with the increase in applied load, as shown in figure 6(b). These results indicate that lubricant D exhibits superb load-carrying capacity, which provides enormous potential in the engineering application involving high load.

3.5. Application in hot steel rolling

Due to the superior tribological performance and load-carrying capacity of lubricant D, its application in hot steel rolling was evaluated in comparison to that of water. Figure 7(a) shows the variation of work roll roughness after rolling with water and lubricant D by turns to compare their lubrication effectiveness. It can be seen clearly that the use of water prompts a decrease in work roll roughness to a certain extent. The subsequent use of lubricant D enables a continuous decrease in work roll roughness. Once the water is reused afterwards, however, the roughness tends to increase instead. On the contrary, the following reuse of lubricant D eventually results in a decreased work roll roughness. These results illustrate that lubricant D has a significant effect on the polishing of work roll surface. The corresponding variation of rolling force obtained under water and lubricant D (see figure 7(b)) is consistent with that of work roll roughness (see figure 7(a)). Specifically, the rolling force can be decreased up to 8.3% when spraying lubricant D onto the polished work roll surface. It is noted that the rolling force varies even though the same lubricant is applied, owing to the different surface conditions of work rolls.

4. Discussion

4.1. Wettability

As one of the most important lubricant characteristics, wettability can be illustrated as a tendency of a lubricant to cover a solid surface [46]. In general, the magnitude of contact angle is used to characterise the wettability, and a smaller contact angle means a better wettability [47]. It has been reported that enhancement of wettability is conductive to the formation of protective film, which can separate the friction pair from direct contact [26, 48].

Figure 8 shows the values of contact angle measured on HSS surface using different lubricants. It reveals that distilled water generates the largest contact angle (73.6°) on HSS surface. The addition of TiO_2 NPs into water (see lubricants A and B) enables an evident decrease in contact angle from 73.6° to 55.2°. In particular, a higher TiO_2 concentration induces a smaller contract angle, which is consistent with the results obtained elsewhere [49, 50]. In another case, the addition of SDBS into lubricants A and B can further decrease the contact angle to 46.6°, suggesting better wettability of lubricant D than that of lubricant C. To explain this phenomenon, the dissociation of SDBS in water produces phenyl sulfonic group that is adsorbed around the NPs, which in turn increases the net negative charge of the NP surface, and therefore increases the repulsive forces between NPs [41]. As a result, the NPs can be well separated with smaller size, exhibiting superior dispersion stability (see figure 3). Meanwhile, smaller size indicates larger surface area, and thus the wettability of nanolubricants can be significantly improved. In addition, increased SDBS tends to largely restrain the agglomeration of NPs, leading to enhanced wettability [42]. As discussed in our previous study [44], the lubricants that have better wettability are inclined to accommodate more effective amounts of TiO_2 NPs adhered onto the work roll surface, and rolling force can thus be reduced due to decreased friction in the contact zone. The tribological performance of the water-based nanolubricants will be discussed next.

4.2. Analysis of worn surface

Figure 9 shows the SEM images of the wear tracks produced after tribological tests using lubricants A and B. It can be observed in figures 9(a) and (c) that there exist TiO_2 NPs which spread over the wear tracks with nearly spherical shapes. In addition, nanoscratches can be found with the width that is close to the diameter of the TiO_2 NPs, and some NPs are deposited in the nanoscratches. The presence of both TiO_2 NPs and nanoscratches hereby reveals the phenomenon of ball-bearing effect [51–53], which is the main cause to reduce the COF and ball wear of using water. The high-resolution SEM images shown in figures 9(b) and (d) indicate that the TiO_2 NPs rolling on the disk with lubricant A are larger than those rolling on the disk with lubricant B. In this regard, the use of lubricant A results in a higher COF and more ball wear than those obtained by using lubricant B due to the agglomeration of NPs [54, 55]. In addition to the comparison of wettability

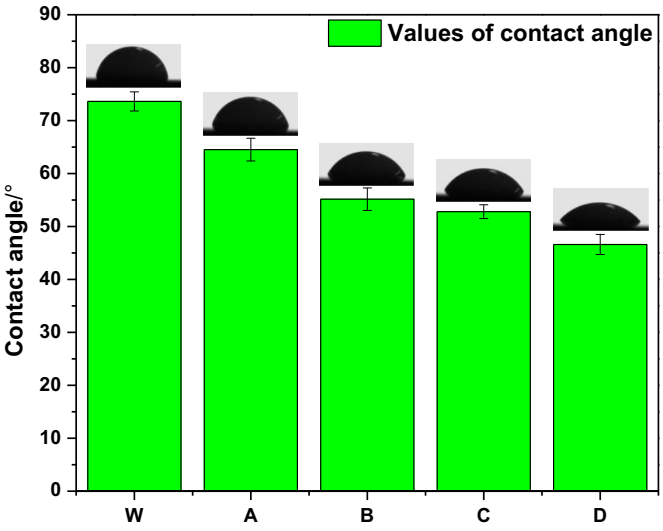

Figure 8. Contact angle values measured on HSS surface using different lubricants.

(see figure 8), lubricant B hence brings forth a lower rolling force than that of lubricant A during hot steel rolling.

Figure 10 presents the SEM images and EDS mappings of the wear tracks produced after tribological tests using lubricants C and D. As can be seen in figure 10(a), there are small island-like nano-TiO_2 films that are distributed on the wear track. The high-resolution SEM image reveals a loose structure of the lubricating film, which separates the ball and disk from direct contact. This nano-TiO_2 lubricating film is supposed to have similar lubrication effect to the protective film formed in the oil-based lubricant, leading to significant decreases in COF and ball wear [56–59]. When the nano-TiO_2 and SDBS concentrations rise to 4 wt% and 0.4 wt%, respectively (see figure 10(b)), block lubricating films with larger sizes can be formed, which may prevent more asperities from contacting each other. Perhaps the primary reason is that the increases in both NPs and SDBS enable the enhancement of wettability, and therefore facilitate the decrease in COF due to the ease of forming lubricating film in the contact area [26, 48]. Another contributing factor is that the addition of SDBS serves the purpose of increasing the viscosity of nanofluids [40], which also results in decreased COF [53]. It is noted that the lubricating film formed is superior to the rolling effect of TiO_2 NPs. Because of this, the lubricants with SDBS (C and D) have better lubrication performance than those without SDBS (A and B).

4.3. Lubrication mechanisms

Prior to the understanding of possible lubrication mechanisms, it is imperative to determine the lubrication regime in the testing condition. As is well-known, there are three types of lubrication regimes as defined from the Stribeck curve, including boundary lubrication, mixed lubrication and hydrodynamic lubrication [7]. The lubrication regime can be approximately determined by the lambda ratio (λ) in equation (1), where λ is the minimum film thickness (h_{min}) in relation to the combined

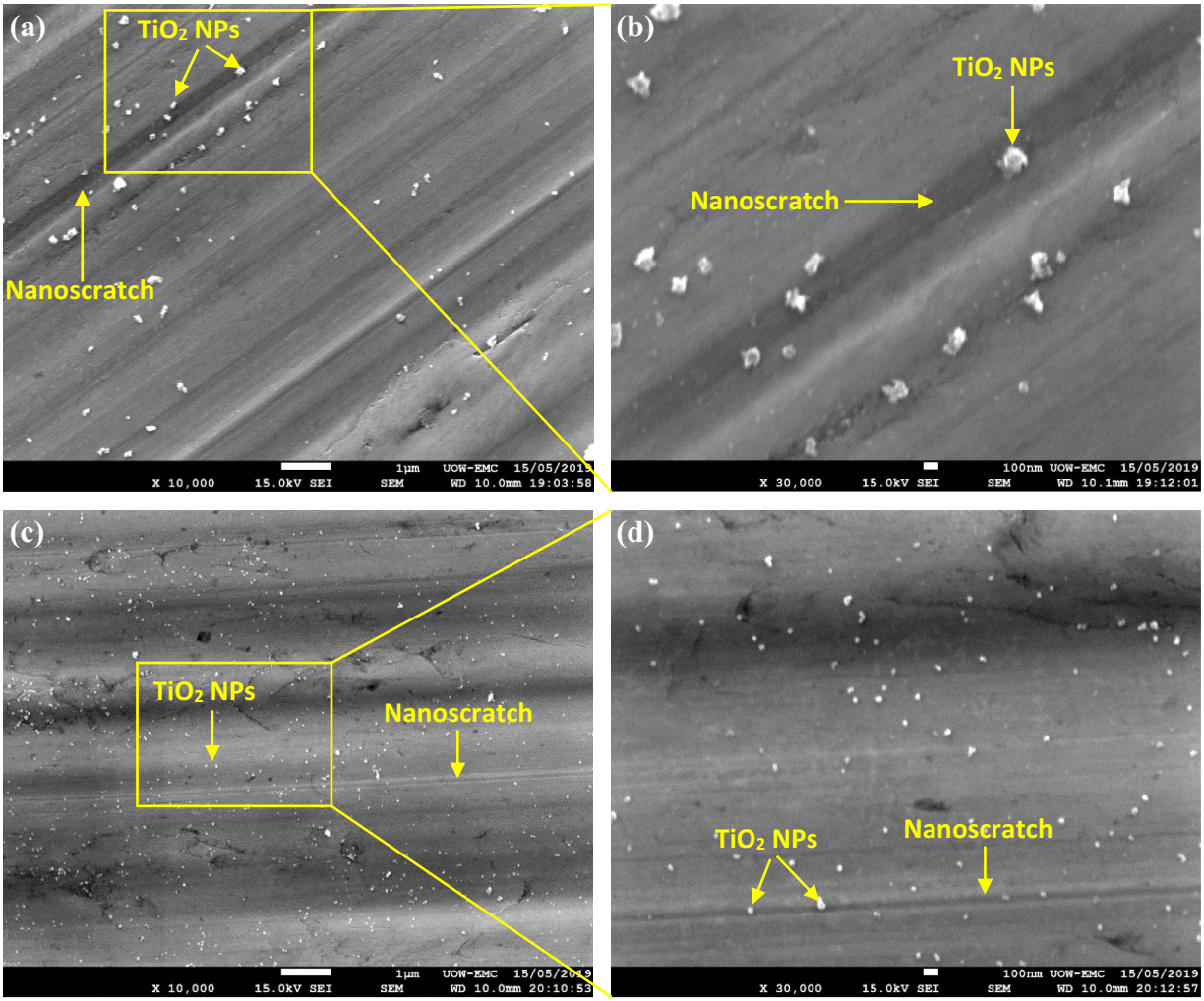

Figure 9. SEM images of the wear tracks produced after tribological tests using (a), (b) lubricant A and (c), (d) lubricant B (30 N, 50 mm s^{-1}, 10 min).

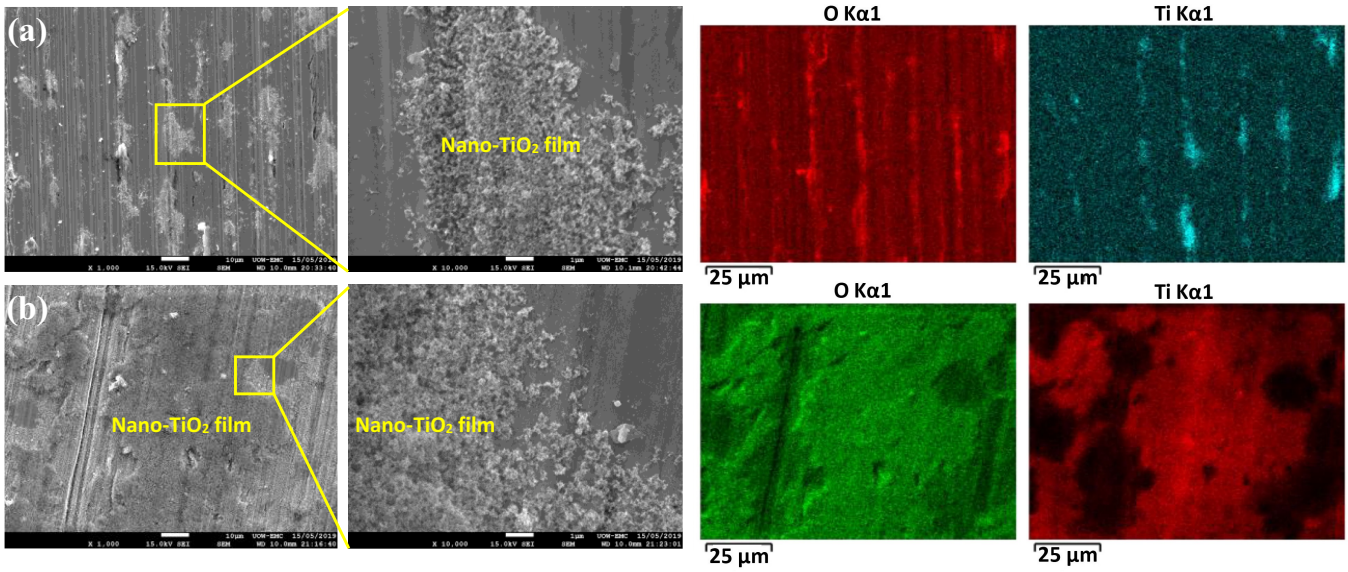

Figure 10. SEM images and EDS mappings of the wear tracks produced after tribological tests using (a) lubricant C and (b) lubricant D (30 N, 50 mm s^{-1}, 10 min).

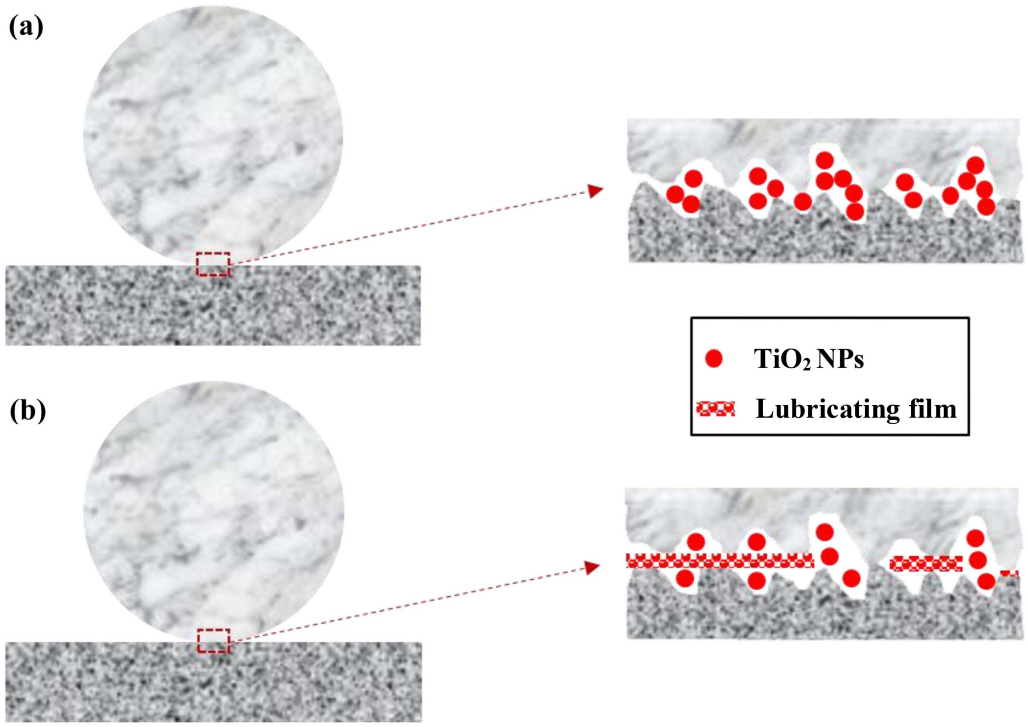

Figure 11. Schematic illustration of the lubrication mechanisms using (a) lubricants A and B, and (b) lubricants C and D.

surface roughness of the friction pair (R_q'). h_{min} can be calculated based on the Hamrock–Dowson model [60], as shown in equation (2). R_q' is calculated following equation (3), in which R_{q1} and R_{q2} are the surface roughness values (R_q) of the ball and disk, respectively.

$$\lambda = h_{min}/R_q' \tag{1}$$

$$h_{min} = 2.8R'(\eta\mu_e/E'R')^{0.65}\left(W_y/E'R'^2\right)^{-0.21} \tag{2}$$

$$R_q' = \sqrt{{R_{q1}}^2 + {R_{q2}}^2} \tag{3}$$

$$1/E\prime = \left(\left(1-V_1^2\right)/E_1 + \left(1-V_2^2\right)/E_2\right)/2, \tag{4}$$

where η is the dynamic viscosity of the lubricant. μ_e is the sliding speed. E' represents the effective elasticity modulus, which can be calculated in equation (4). Therein, E_1, V_1 and E_2, V_2 are the Young's modulus and Poisson ration of the ball and disk, respectively. R' is the radius of the ball. W_y indicates the normal load applied on the Cr steel ball. It has been reported that boundary lubrication occurs if λ is lower than one; mixed lubrication exists when λ ranges from 1 to 3; the value of λ above three corresponds to hydrodynamic lubrication [26]. Calculated from equations (1)–(4), the minimum film thickness obtained when using lubricants A, B, C, and D is approximately 0.463, 0.488, 0.482 and 0.622 nm under the lubrication conditions shown in figure 4 (30 N, 50 mm s^{-1}, 10 min). The corresponding values of λ obtained by using lubricants A, B, C and D are about 0.0026, 0.0027, 0.0027 and 0.0034, respectively, all indicating a boundary lubrication regime in the contact zone. Under varying loads from 20 to 80 N, the lubrication regime of using lubricant D can also be determined as boundary lubrication. Together with the results obtained in figures 9 and 10, the lubrication model of the water-based nanolubricants is schematically illustrated in figure 11. For the water-based nanolubricants without SDBS (see figure 11(a)), the TiO_2 NPs act as ball bearings that can roll in the contact zone between the Cr steel ball and the Q345 disk. As a result, some peaks of asperities on the surfaces of the ball and disk can be separated, while some other peaks can still contact each other due to limited film thickness. When SDBS is added into the nanolubricant, in contrast, both the wettability and the viscosity can be enhanced, which promotes the formation of lubricating films, as shown in figure 11(b). This greatly helps increase the film thickness, and therefore further restrain the friction pair from contacting each other, leading to decreased COF and ball wear to a large extent. There should be an emphasis on the best lubrication effectiveness using lubricant D, which is mainly attributed to the increases in both thickness and size of the lubricating film. Therefore, it is expected that lubricant D has great potential to be successfully applied in practical hot steel rolling by largely decreasing rolling force and wear of work rolls.

5. Conclusions

In this study, the tribological performance and rolling lubrication properties of novel water-based nanolubricants were

investigated using a ball-on-disk tribometer and a 2-high Hille 100 experimental rolling mill. The main conclusions can be drawn below.

(a) The as-synthesised water-based nanolubricants exhibited excellent dispersion stability and wettability.
(b) The water-based nanolubricant without SDBS showed moderate lubrication effectiveness on the reduction of COF and ball wear, owing to the ball-bearing effect of TiO_2 NPs.
(c) The water-based nanolubricant containing 4 wt% TiO_2 and 0.4 wt% SDBS exhibited superior tribological performance by decreasing COF and ball wear up to 70.5% and 84.3%, respectively, compared to those of pure water, due to the formation of nano-TiO_2 lubricating films.
(d) The use of water-based nanolubricant containing 4 wt% TiO_2 and 0.4 wt% SDBS had significant effect on polishing of the work roll surface, and thus decreased the rolling force up to 8.3% at a rolling temperature of 850 °C with a workpiece reduction of 30%.
(e) The lubrication performance was significantly improved with transition from ball-bearing effect to lubricating film by adding SDBS into TiO_2 water-based nanolubricant, and a boundary lubrication regime was confirmed during tribological and hot steel rolling tests.

Acknowledgments

The authors acknowledge the financial supports from Baosteel-Australia Joint Research & Development Center (BAJC) under the project of BA17004 and Australian Research Council (ARC) under Linkage Project Program (LP150100591). The authors are grateful to Mr Suoquan Zhang and Mr Zhao Xing at Baosteel Research Institute for the provision of steel samples. The authors wish to thank the technicians in the workshop of SMART Infrastructure Facility at University of Wollongong for their great support on samples machining. The authors also wish to extend special thanks to Dr Klaudia Wagner in the measurement of contact angle. Finally, the authors would like to acknowledge the Australian National Fabrication Facility (ANFF)—Materials node for providing instrumentation.

ORCID iD

Hui Wu https://orcid.org/0000-0002-3322-5324

References

[1] Yu X L, Zhou J and Jiang Z Y 2016 Developments and possibilities for nanoparticles in water-based lubrication during metal processing *Rev. Nanosci. Nanotechnol.* **5** 136–63
[2] Hao L, Wu H, Wei D B, Cheng X W, Zhao J W, Luo S, Jiang L and Jiang Z 2017 Wear and friction behaviour of high-speed steel and indefinite chill material for rolling ferritic stainless steels *Wear* **376–7** 1580–5
[3] Xie H B, Jiang Z Y and Yuen W Y D 2011 Analysis of friction and surface roughness effects on edge crack evolution of thin strip during cold rolling *Tribol. Int.* **44** 971–9
[4] Jiang Z Y, Xiong S W, Tieu A K and Wang Q J 2008 Modelling of the effect of friction on cold strip rolling *J. Mater. Process. Technol.* **201** 85–90
[5] Fu Y Q, Batchelor A W, Loh N K and Tan K W 1998 Effect of lubrication by mineral and synthetic oils on the sliding wear of plasma nitrided AISI 410 stainless steel *Wear* **219** 169–76
[6] Haus F, German J and Junter G A 2001 Primary biodegradability of mineral base oils in relation to their chemical and physical characteristics *Chemosphere* **45** 983–90
[7] Sotres J and Arnebrant T 2013 Experimental investigations of biological lubrication at the nanoscale: the cases of synovial joints and the oral cavity *Lubricants* **1** 102–31
[8] Dubey S P, Sharma G K, Shishodia K S and Sekhon G S 2005 Study on the performance of oil-in-water emulsions during cold rolling of steel strip *Tribol. Trans.* **48** 499–504
[9] Hu X G, Wang R and Jing H F 2010 Application of oil-in-water emulsion in hot rolling process of brass sheet *Ind. Lubr. Tribol.* **62** 224–31
[10] Xia W Z, Zhao J W, Wu H, Jiao S H, Zhao X M, Xhu J H and Jiang Z 2018 Analysis of oil-in-water based nanolubricants with varying mass fractions of oil and TiO_2 nanoparticles *Wear* **396–7** 162–71
[11] Xia W Z, Zhao J W, Wu H, Jiao S H and Jiang Z Y 2017 Effects of oil-in-water based nanolubricant containing TiO_2 nanoparticles on the tribological behaviour of oxidised high-speed steel *Tribol. Int.* **110** 77–85
[12] Xia W Z *et al* 2018 Effects of oil-in-water based nanolubricant containing TiO_2 nanoparticles in hot rolling of 304 stainless steel *J. Mater. Process. Technol.* **262** 149–56
[13] Özerinç S, Kakaç S and Yazıcıoğlu A G 2010 Enhanced thermal conductivity of nanofluids: a state-of-the-art review *Microfluid. Nanofluid.* **8** 145–70
[14] Zhao J H, Yang G B, Zhang C L, Zhang Y J, Zhang S M and Zhang P Y 2019 Synthesis of water-soluble Cu nanoparticles and evaluation of their tribological properties and thermal conductivity as a water-based additive *Friction* **7** 246–59
[15] Song H J, Huang J, Jia X H and Sheng W C 2018 Facile synthesis of core–shell Ag@C nanospheres with improved tribological properties for water-based additives *New J. Chem.* **42** 8773–82
[16] Pardue T N, Acharya B, Curtis C K and Krim J 2018 A tribological study of γFe_2O_3 nanoparticles in aqueous suspension *Tribol. Lett.* **66** 130
[17] Meng Y N, Sun J L, Wu P, Dong C and Yan X D 2018 The role of nano-TiO_2 lubricating fluid on the hot rolled surface and metallographic structure of SS41 steel *Nanomaterials* **8** 111
[18] He A S, Huang S Q, Yun J H, Wu H, Jiang Z Y, Stokes J, Jiao S, Wang L and Huang H 2017 Tribological performance and lubrication mechanism of alumina nanoparticle water-based suspensions in ball-on-three-plate testing *Tribol. Lett.* **65** 40
[19] Ding M, Lin B, Sui T Y, Wang A Y, Yan S and Yang Q 2018 The excellent anti-wear and friction reduction properties of silica nanoparticles as ceramic water lubrication additives *Ceram. Int.* **44** 14901–6
[20] Bao Y Y, Sun J L and Kong L H 2017 Effects of nano-SiO_2 as water-based lubricant additive on surface qualities of strips after hot rolling *Tribol. Int.* **114** 257–63
[21] Zhao J H, Yang G B, Zhang Y J, Zhang S M and Zhang P Y 2019 A simple preparation of HDA-CuS nanoparticles and their tribological properties as a water-based lubrication additive *Tribol. Lett.* **67** 88

[22] Wang Y X, Du Y Y, Deng J A and Wang Z P 2019 Friction reduction of water based lubricant with highly dispersed functional MoS_2 nanosheets *Colloids Surf.* A **562** 321–8

[23] Lin B, Ding M, Sui T Y, Cui Y X, Yan S and Li X 2019 Excellent water lubrication additives for silicon nitride to achieve superlubricity under extreme conditions *Langmuir* **35** 14861–9

[24] He J Q, Sun J L, Meng Y N and Yan X D 2019 Preliminary investigations on the tribological performance of hexagonal boron nitride nanofluids as lubricant for steel/steel friction pairs *Surf. Topogr.: Metrol. Prop.* **7** 015022

[25] Cho D H, Kim J S, Kwon S H, Lee C and Lee Y Z 2013 Evaluation of hexagonal boron nitride nano-sheets as a lubricant additive in water *Wear* **302** 981–6

[26] Xie H M, Dang S H, Jiang B, Xiang L, Zhou S, Sheng H, Yang T and Pan S 2019 Tribological performances of SiO_2/graphene combinations as water-based lubricant additives for magnesium alloy rolling *Appl. Surf. Sci.* **475** 847–56

[27] Wu P, Chen X C, Zhang C H and Luo J B 2019 Synergistic tribological behaviors of graphene oxide and nanodiamond as lubricating additives in water *Tribol. Int.* **132** 177–84

[28] Huang S Q, He A S, Yun J H, Xu X F, Jiang Z Y, Jiao S and Huang H 2019 Synergistic tribological performance of a water based lubricant using graphene oxide and alumina hybrid nanoparticles as additives *Tribol. Int.* **135** 170–80

[29] He A S, Huang S Q, Yun J H, Jiang Z Y, Stokes J R, Jiao S, Wang L and Huang H 2018 Tribological characteristics of aqueous graphene oxide, graphitic carbon nitride, and their mixed suspensions *Tribol. Lett.* **66** 42

[30] Huang S Q, Li X L, Yu B W, Jiang Z Y and Huang H 2020 Machining characteristics and mechanism of GO/SiO_2 nanoslurries in fixed abrasive lapping *J. Mater. Process. Technol.* **277** 116444

[31] Ye X Y, E S F and Fan M J 2019 The influences of functionalized carbon nanotubes as lubricating additives: length and diameter *Diam. Relat. Mater.* **100** 107548

[32] Tang W W, Wang B G, Li J T, Li Y Z, Zhang Y, Quang H and Huang Z 2019 Facile pyrolysis synthesis of ionic liquid capped carbon dots and subsequent application as the water-based lubricant additives *J. Mater. Sci.* **54** 1171–83

[33] Shariatzadeh M and Grecov D 2019 Aqueous suspensions of cellulose nanocrystals as water-based lubricants *Cellulose* **26** 4665–77

[34] He A S, Huang S Q, Yun J H, Jiang Z Y, Stokes J, Jiao S, Wang L and Huang H 2017 The pH-dependent structural and tribological behaviour of aqueous graphene oxide suspensions *Tribol. Int.* **116** 460–9

[35] Dai W, Kheireddin B, Gao H and Liang H 2016 Roles of nanoparticles in oil lubrication *Tribol. Int.* **102** 88–98

[36] Wu H *et al* 2018 Friction and wear characteristics of TiO_2 nano-additive water-based lubricant on ferritic stainless steel *Tribol. Int.* **117** 24–38

[37] Wu H, Jia F H, Zhao J W, Huang S Q, Wang L Z, Jiao S, Huang H and Jiang Z 2019 Effect of water-based nanolubricant containing nano-TiO_2 on friction and wear behaviour of chrome steel at ambient and elevated temperatures *Wear* **426–7** 792–804

[38] Wu H *et al* 2017 A study of the tribological behaviour of TiO_2 nano-additive water-based lubricants *Tribol. Int.* **109** 398–408

[39] Wu H, Li Y, Lu Y, Li Z, Cheng X W, Hasan M, Zhang H and Jiang Z 2019 Influences of load and microstructure on tribocorrosion behaviour of high strength hull steel in saline solution *Tribol. Lett.* **67** 124

[40] LotfizadehDehkordi B, Kazi S N, Hamdi M, Ghadimi A Sadeghinezhad E and Metselaar H S C 2013 Investigation of viscosity and thermal conductivity of alumina nanofluids with addition of SDBS *Heat Mass Transfer* **49** 1109–15

[41] Wang X J, Zhu D S and Yang S 2009 Investigation of pH and SDBS on enhancement of thermal conductivity in nanofluids *Chem. Phys. Lett.* **470** 107–11

[42] Wang B X, Zhao Y and Zhao X P 2007 The wettability, size effect and electrorheological activity of modified titanium oxide nanoparticles *Colloid Surf.* A **295** 27–33

[43] Wu H, Zhao J W, Luo L, Huang S Q, Wang L Z, Zhang S Q, Jiao S, Huang H and Jiang Z 2018 Performance evaluation and lubrication mechanism of water-based nanolubricants containing nano-TiO_2 in hot steel rolling *Lubricants* **6** 57

[44] Wu H *et al* 2017 Analysis of TiO_2 nano-additive water-based lubricants in hot rolling of microalloyed steel *J. Manuf. Process.* **27** 26–36

[45] Wu H, Jiang C Y, Zhang J Q, Huang S Q, Wang L Z, Jiao S, Huang H and Jiang Z 2019 Oxidation behaviour of steel during hot rolling by using TiO_2-containing water-based nanolubricant *Oxid. Met.* **92** 315–35

[46] Pawlak Z, Urbaniak W and Oloyede A 2011 The relationship between friction and wettability in aqueous environment *Wear* **271** 1745–9

[47] Anderson W 1986 Wettability literature survey-part 2: wettability measurement *J. Pet. Technol.* **38** 1246–62

[48] Liang S S, Shen Z G, Yi M, Liu L, Zhang X J and Ma S 2016 In-situ exfoliated graphene for high-performance water-based lubricants *Carbon* **96** 1181–90

[49] Vafaei S, Borca-Tasciuc T, Podowski M Z, Purkayastha A, Ramanath G and Ajayan P M 2006 Effect of nanoparticles on sessile droplet contact angle *Nanotechnology* **17** 2523

[50] Xia W Z, Zhao J W, Wu H, Zhao X M, Zhang X M, Xu J H, Hee A C and Jiang Z 2017 Effects of nano-TiO_2 additive in oil-in-water lubricant on contact angle and antiscratch behavior *Tribol. Trans.* **60** 362–72

[51] Rapoport L, Leshchinsky V, Lvovsky M, Lapsker I, Volovik Y, Feldman Y, Popovitz-Biro R and Tenne R 2003 Superior tribological properties of powder materials with solid lubricant nanoparticles *Wear* **255** 794–800

[52] Xu T, Zhao J Z and Xu K 1996 The ball-bearing effect of diamond nanoparticles as an oil additive *J. Phys. D: Appl. Phys.* **29** 2932

[53] Wu Y Y, Tsui W C and Liu T C 2007 Experimental analysis of tribological properties of lubricating oils with nanoparticle additives *Wear* **262** 819–25

[54] Jiao D, Zheng S H, Wang Y Z, Guan R F and Cao B Q 2011 The tribology properties of alumina/silica composite nanoparticles as lubricant additives *Appl. Surf. Sci.* **257** 5720–5

[55] Su Y, Gong L and Chen D D 2015 An investigation on tribological properties and lubrication mechanism of graphite nanoparticles as vegetable based oil additive *J. Nanomater.* **16** 203

[56] Hu Z S, Lai R, Lou F, Wang L G, Chen Z L, Chen G X and Dong J X 2002 Preparation and tribological properties of nanometer magnesium borate as lubricating oil additive *Wear* **252** 370–4

[57] Ji X B, Chen Y X, Zhao G Q, Wang X B and Liu W M 2011 Tribological properties of $CaCO_3$ nanoparticles as an additive in lithium grease *Tribol. Lett.* **41** 113–9

[58] Rapoport L, Leshchinsky V, Lapsker I, Volovik Y, Nepomnyashchy O, Lvovsky M, Popovitz-Biro R, Feldman Y and Tenne R 2003 Tribological properties of WS_2 nanoparticles under mixed lubrication *Wear* **255** 785–93

[59] Rastogi R B, Yadav M and Bhattacharya A 2002 Application of molybdenum complexes of 1-aryl-2,5-dithiohydrazodicarbonamides as extreme pressure lubricant additives *Wear* **252** 686–92

[60] Hamrock B J, Schmid S R and Jacobson B O 2004 *Fundamentals of Fluid Film Lubrication* 2nd edn (New York: CRC Press)